

Oxidation of cyanobactin precursor peptide is independent of leader peptide and operates in a defined order.

Sisi Gao^{‡1,2}, Ying Ge^{‡1}, Andrew F Bent^{1^}, Ulrich Schwarz-Linek¹, James H Naismith^{2,3*}

¹ Biomedical Sciences Research Complex, University of St Andrews, St Andrews, Fife KY16 9ST UK

² Research Complex at Harwell, Didcot, Oxon, OX11 0FA UK

³ Division of Structural Biology, University of Oxford, Oxford, OX3 7BN UK

[^] Deceased

* To whom correspondence should be addressed

‡ These authors contributed equally to the work

KEYWORDS Oxidation, enzyme, macrocycles, azoles, azoline

Supporting Information Placeholder

ABSTRACT: The five-membered nitrogen plus heteroatom rings known as azolines or in their oxidised form as azoles are very common in natural products and drugs. The oxidation of thiazoline to thiazole in the cyanobactin class of natural products is one of several important transformations which is known to alter the biological properties of the compound. The ordering of the various chemical reactions that occur during cyanobactin biosynthesis is not fully understood. The structure of the flavin-dependent enzyme responsible for the oxidation of multiple thiazolines reveals it contains an additional domain that in other enzymes recognises linear peptides. We characterise the enzyme activity of the oxidase on two substrates – one with a peptide leader and one without. Kinetics and biophysics reveal that the leader on substrate is not recognised by the enzyme. The oxidase enzyme is faster on either substrate than the macrocyclase or protease *in vitro*. The enzyme has a preferred order of oxidation of multiple thiazolines in the same linear peptide.

Introduction

Cyclic peptides have come under intensive investigation in recent years due to the bioactivities they possess, including anticancer,¹ antibacterial² and immuno-suppressive.³ Reduced structural flexibility⁴ gives cyclic peptides higher receptor binding affinity than their linear counterparts through a lower entropic penalty upon binding.⁵ Cyanobactins⁶ are a class of macrocyclic compounds, produced by cyanobacteria, and often contain

posttranslational modifications including five-membered rings (azolines and azoles⁷) that are produced from cysteine, threonine or serines.⁸ Thiazolines, methyloxazolines and oxazolines are made by a heterocyclase, and can undergo enzymatic oxidation to become thiazoles and (methyl)oxazoles, respectively.⁹ Azoles are aromatic, chemically more stable, and conformationally different from azolines due to the flattening of the ring.¹⁰ The oxidation status of thiazoline/oxazoline is known to alter the function of the parent macrocycles.¹¹ The most striking demonstration is an increase of two orders of magnitude in cytotoxicity against bladder carcinoma cells between lissoclinamides 4 and 5 (Figure 1) which differ only in thiazoline vs thiazole.¹²

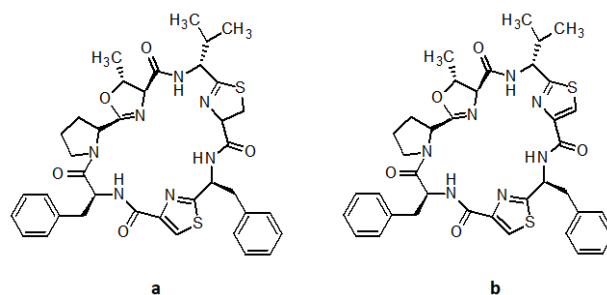


Figure 1 Structure of lissoclinamides. a. lissoclinamide 4 b. lissoclinamide 5. Their difference is highlighted in blue.

Azol(ine)s are commonly found in ribosomally synthesized and posttranslationally modified peptides (RiPPs)

of the thiazole/oxazole-modified microcins (TOMMs) class.¹³ Microcin B17 is a classic TOMM peptide, and azoles are produced by the McbBCD complex which is comprised of a recognition domain (peptide clamp, also termed the RiPP domain)¹⁴, a heterocyclase (cyclodehydratase) and an oxidase (dehydrogenase).¹⁵ BalhBCD, another TOMM biosynthetic enzyme, also operates as a tripartite complex.¹⁶ In contrast, the cyanobactin oxidase does not appear to form a complex with the heterocyclase, which in cyanobactin biosynthetic pathways is found as a fusion of the RiPP domain and the YcaO (catalytic) domain. The oxidase is either fused with the macrocyclase enzyme and a domain of unknown function, or found as a standalone protein. In addition, the cyanobactin oxidases have two RiPP domains at the N-terminus, shown by the crystal structure of ThcOx (Figure 2b) from the cyanothecamide biosynthesis pathway.¹⁷ The C-terminal domain shows sequence homology to other TOMM oxidases and binds flavin mononucleotide (FMN), identifying it as the catalytic domain. The functions of the RiPP domains in ThcOx, which share high structural similarity with the leader-binding domain in LynD¹⁸ (Figure S1), are however poorly understood. The second of the two domains sits at the dimer with the clamping region hidden, whereas the clamp region of the N-terminal RiPP domain is exposed and may participate in substrate binding (Figure 2b)¹⁴

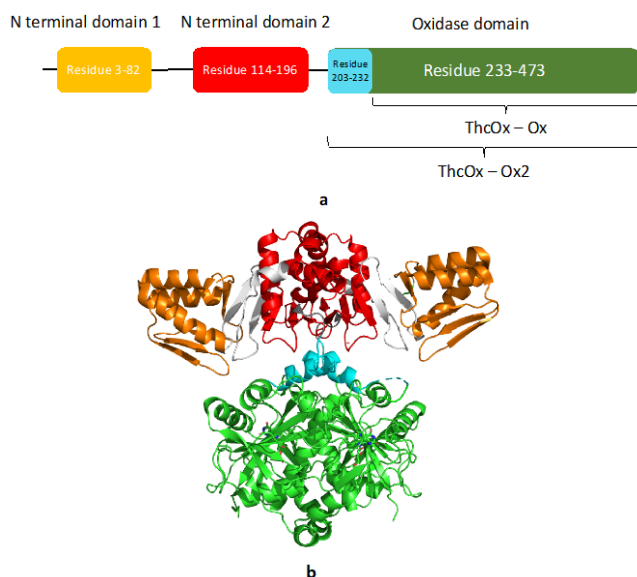


Figure 2 Crystal structure and schematic representation of ThcOx. N-terminal RiPP domains are coloured in orange and red; the linker in grey. The oxidase domain is coloured in green and cyan, to illustrate the truncations made. ThcOx-Ox2 contains residues 203-473 (cyan and green), while ThcOx-Ox contains only residues 233-473 (green).

Here we report the first biochemical characterisation of a cyanobactin-type oxidase. We showed that the oxidases ThcOx and ArtGox operate on leaderless and full-length

linear peptide substrates. We have determined that the reaction proceeds with an order where there are multiple thiazolines in the substrate, and that the order is preserved irrespective whether the leader peptide is present. Despite the presence of RiPP domains, no interaction was found between the leader peptide and the oxidase. The N-terminal domains instead appear to maintain the structural integrity and consequently activity of the enzyme as a whole.

Materials and Methods

General methods. Unless specified, all chemicals were purchased from Sigma-Aldrich or Fisher Scientific. Oligonucleotides were purchased from ThermoFisher Scientific. Restriction enzymes were purchased from Promega. dNTP and DNA polymerase were purchased from EMD Millipore™ Novagen™ KOD Hot Start DNA Polymerase kit. DNA sequencing was performed by GATC. Peptides were purchased from Biosynthesis.

Cloning and overexpression. ThcOx (*Cyanothece* sp. PCC 7425, UniprotKB B8HTZ1) was expressed with an N-terminal *Tobacco etch virus* (TEV) protease-cleavable His₆ tag followed by a four-glycine as previously described.¹⁹ ArtGox (*Arthrospira platensis*, UniprotKB H1W8K1)¹⁹ was cloned into a pEHISTEVSUMO vector,²⁰ and expressed with an N-terminal His₆ tag followed by a SUMO tag and TEV protease cleavage site. ThcOx-Ox (residue 233-473 of ThcOx) and ThcOx-Ox2 (residue 203-473) were cloned from full length ThcOx into a pEHISTEV vector with a N terminal His₆-tag and a TEV protease cleavage site.²⁰ All proteins were expressed in *Escherichia coli* BL21 (DE3) cells grown in autoinduction medium by Studier method for 48 hours at 20°C.²¹ For ArtGox, ThcOx and variants, 50μM riboflavin was added to the expression media.

PatE3', PatE3KK and ThcE1 (Figure S2 gives sequences) were cloned into a pBMS23CHIS vector²⁰ and expressed with a C-terminal non-cleavable His₆ tag in *E.coli* BL21(DE3) cells. Starter cultures were grown in LB media at 37 °C, 200 rpm until the optical density at the wavelength of 600 nm reaches 0.6, and induced with 1 mM IPTG. Cells were further incubated at 37 °C, 200 rpm for 5 hours before harvesting by centrifugation at 4000 rpm for 15 min at 20 °C. u-¹³C, ¹⁵N-labelled and u-¹⁵N-labelled PatE2K were expressed as previously described.²²

Purification of proteins and peptides.

E. coli cells overexpressing ThcOx, ArtGox and ThcOx-Ox were resuspended in lysis buffer (150 mM NaCl, 20 mM Tris-HCL pH 8.0, 20 mM imidazole pH 8.0, 50 μM

FMN, 3 mM 2-mercaptoethanol) plus EDTA-free protease-inhibitor tablets (Roche) and DNase at 0.4mg per gram of wet cell pellet. The resuspension was lysed by passing through a cell disruptor at 30 kpsi (Constant systems). The lysate was cleared by centrifugation (6,000 rpm, 4 °C, 20 min) and then loaded onto a Ni Sepharose 6 Fast Flow column (GE Healthcare) equilibrated with lysis buffer. The protein was eluted with elution buffer (150 mM NaCl, 20 mM Tris-HCL pH 8.0, 250 mM imidazole pH 8.0, 50 μ M FMN, 3 mM 2-mercaptoethanol) and passed over a desalting column (16/10 Desalting, GE Healthcare) exchanging into the desalting buffer (100 mM NaCl, 20 mM Tris-HCL pH 8.0, 3 mM 2-mercaptoethanol, 50 μ M FMN). TEV protease was added at a mass ratio of 1:10 and the protein was digested for 3 hours at 20 °C before being loaded onto a second nickel column pre-equilibrated with desalting buffer. The eluted protein was applied directly to an anion-exchange column (HisTrap Q Sepharose FF, GE Healthcare) where it was eluted with a 0.1 to 1 M NaCl gradient. The peak fraction was then concentrated to 7.5 ml (Vivaspin concentrators, 30 kDa MWCO) and applied onto a Superdex 200 gel filtration column (GE Healthcare) equilibrated with gel filtration buffer (150 mM NaCl, 20 mM HEPES pH 7.4, 1 mM TCEP). Heterocyclases LynD (UniprotKB A0YXD2), AcLynD and MicD (UniprotKB I4F6C3) were purified as previously described.^{18, 19}

Cells expressing precursor peptides were re-suspended in urea lysis buffer (8 M Urea, 500 mM NaCl, 20 mM Tris-HCL pH 8.0, 20 mM imidazole pH 8.0, 3 mM 2-mercaptoethanol) and lysed by sonication then the lysate cleared by centrifugation at 19,000 rpm for 20 min at 20 °C. The supernatant was filtered through 5 μ m and 0.8 μ m filters before being loaded onto a Ni-Sepharose 6 FF column (GE Healthcare) pre-equilibrated with lysis buffer. Peptide was eluted with urea elution buffer (8 M Urea, 500 mM NaCl, 20 mM Tris-HCL pH 8.0, 250 mM imidazole pH 8.0, 3 mM 2-mercaptoethanol). The eluate was supplemented with 10 mM dithiothreitol (DTT) and incubated at 20 °C for 2 hours to reduce all the cysteines. PatE3' was subjected to size-exclusion chromatography (Superdex 75, GE Healthcare) in gel filtration buffer (150mM NaCl, 20mM HEPES). The integrity, identity and purity of the proteins and peptides was confirmed by SDS-PAGE and mass spectrometry.

Heterocyclisation and Proteolysis. To produce substrates with thiazoline heterocycles for oxidation (Scheme S1), 100 μ M PatE3' or ThcE1 was reacted with MicD (10 μ M), in gel filtration buffer (150 mM NaCl, 20 mM HEPES, 1 mM TCEP) supplemented with MgCl₂ (10 mM) and ATP (10 mM), at 27 °C for 16 hours. ¹⁵N E2K (175 μ M) was reacted with LynD (5 μ M), and PatE3KK was reacted with MicD (10 μ M) for 16 h at room temperature, in 100 mM Tris pH 8.0 supplemented with 150 mM

NaCl, 10 mM ATP, 10 mM MgCl₂ and 5 mM DTT. The reaction mixtures were then loaded onto a Superdex 75 column (GE Healthcare), equilibrated in gel filtration buffer to separate MicD/LynD and the heterocyclised material (Figure S3). Heterocyclisation of these substrates was confirmed by MS (Figure S4, S6).

Where leaderless substrates were used, heterocyclised peptides were incubated with trypsin (1:100 mass ratio) at 20 °C for 16 hours to cleave the leader. In the case of PatE2K and PatE3', the trypsin-treated sample was loaded onto a Ni-Sepharose 6 FF column (GE Healthcare), pre-equilibrated with gel filtration buffer. The eluate was then passed through a desalting column (16/10 Desalting, GE Healthcare) into gel filtration buffer. Proteolysis was confirmed by MS (Figure S5, S7). In the case of PatE3KK, trypsin was inactivated by heating the sample at 100 °C for 10 min, and no purification step was carried out. Finally, the chemically synthesized peptide ITACITFCAYD (Biosynthesis) was incubated with AcLynD (10 μ M) in gel filtration buffer supplemented with 10 mM ATP and 10 mM MgCl₂ for 16 h at 20 °C, prior to reaction with ThcOx and variants (10 μ M each), without purification in between.

Oxidation reactions. Various concentrations of enzymes and substrates were used as stated individually in the results section. ThcOx reactions were carried out in 100 mM HEPES pH 7.5, 150mM NaCl. ArtGox reactions were carried out in 100 mM Tris pH 8.0 supplemented with 150 mM NaCl and 2mM FMN.

Enzyme Kinetics. Steady-state kinetics were obtained using a commercial hydrogen peroxide assay kit (Abcam, ab102500). ThcOx (100 nM, Figure S8) and varying concentrations of heterocycle containing full-length and leaderless PatE3' or full-length ThcE1. The substrates were added to a Corning™ 96-well half area black flat bottom polystyrene microplate. In the presence of Horse Radish Peroxidase (HRP), the OxiRed probe produces a product with red fluorescent (Ex/Em=535/587 nm) by reaction with H₂O₂, which is the other of azole formation (Scheme S2). Fluorescence was measured with a Spectra-Max 2e microplate reader (Molecular Devices). All experiments were performed at 25 °C. Data were corrected for the auto-fluorescence of ThcOx and the substrate were used for background correction. Initial rates were plotted against substrate concentration and fitted to the Michaelis-Menton Equation (below) in Graphpad Prism.

$$v_{int} = \frac{V_{max}[S]}{K_m + [S]}$$

Biophysics. ITC experiments were carried out on a Malvern Panalytical MicroCal iTC200 MicroCalorimeter. A cell concentration of 20 μ M ThcOx with a syringe concentration of 400 μ M PatE3' and ThcE1 was added into

the system. Both the substrate and ThcOx were in gel filtration buffer.

ThcOx-Ox was subjected to the size exclusion chromatography multi-angle light scattering (SEC-MALS)²³ for determination of molecular mass. Purified protein was loaded onto a GE Health Superdex 200 column, equilibrated in Gel filtration buffer (150mM NaCl, 10mM HEPES, 1mM TCEP), attached to the Wyatt Dawn Heleos II Multi-Angle Light Scattering detector and Wyatt Optilab T-rex Refractive Index detector. Protein elution peak was recorded by differential refractive index (dRI).

ThcOx-Ox was exchanged into circular dichroism buffer (500 mM sodium phosphate buffer pH 8.0, 200 mM NaF) and concentrated to a final concentration of 0.2 mg/ml. The circular dichroism signal was measured and recorded by a Bio-Logic Science Instrument MOS-500 Circular Dichroism Spectrometer.

¹H, ¹⁵N HSQC spectra of full-length u-¹³C, ¹⁵N PatE2K were acquired on a Bruker AVANCE 500 MHz spectrometer equipped with a TXIz probe, controlled by Bruker Topspin software. A standard Bruker pulse sequence with Watergate water suppression was used with 8 transients at 2048×128 points with spectral resolutions of 9.8 Hz and 19.0 Hz in the direct (¹H) and indirect (¹⁵N) dimensions, respectively. HSQC spectra were also recorded at 10 °C for the starting material, and 12 h and 60 h after the addition of 10 μM ArtGox. For sequential assignment, HNCACB spectra were acquired with 16 transients at 1024×50×128 points and spectral resolutions of 13.7 Hz, 44.6 Hz, and 157.1 Hz for the ¹H, ¹⁵N and ¹³C dimensions, respectively. CBCA(CO)NH spectra were acquired with 8 transients at 1024×50×114 points and spectral resolutions of 13.7 Hz, 44.6 Hz, and 176.4 Hz for the ¹H, ¹⁵N and ¹³C dimensions, respectively. Equivalent spectra were recorded for fully oxidized u-¹³C, ¹⁵N -PatE-2het (concentration 1.0 mM) and a sample where the enzymatic transformation was interrupted after 12 h by gel filtration on a Superdex S75 column (GE Healthcare) in heterocyclisation buffer supplemented with 5 mM FMN, thus allowing assignment of the reaction intermediate.

NMR experiments with the leaderless substrate were performed at 20 °C on a Bruker Ascend 700 MHz spectrometer equipped with a Prodigy TCI probe, controlled by Bruker Topspin software. For oxidation monitoring, 0.2 M cleaved peptide (see Preparation of Leaderless Substrate) was reacted with 10 μM ArtGox in 10 mM HEPES pH 7.4, 150 mM NaCl, 5 mM FMN and 5% D₂O at 20 °C. ¹H, ¹⁵N HSQC spectra were recorded before the addition of enzyme, 5 min and 20 min afterwards, and then every 30 min. Six transients were recorded at 1536×80 points with spectral resolutions of 12.8 Hz and 26.6 Hz in the direct (¹H) and indirect (¹⁵N) dimensions, respectively. ¹H, ¹⁵N HSQC spectra were recorded at 10

°C for the unreacted substrate and the final product. Sequential assignment of the full-length peptide was transferred to the ¹H, ¹⁵N HSQC spectrum at 10 °C and then to the corresponding spectrum at 20 °C. Raw spectral data were processed by Topspin and analysed with CCPN Analysis 2.²¹

Results

The Cyanobactin Oxidase operates on both full length and ‘leaderless’ substrates but is faster on ‘leaderless’ substrates

The presence of RiPP domains in the cyanobactin oxidase, along with the fact that crystals were only obtained when the peptide NILPQQGQPVR was added¹⁷, led to the hypothesis that parts of the leader peptide are involved in enzyme-substrate interaction. We predicted inactivity or reduced activity against leaderless peptides would be observed if the leader was important. ArtGox, previously been shown to oxidise thiazolines in full-length (leader-containing) peptides,¹⁹ was reacted with the four heterocycle containing peptide IT^{het}AC^{het}IT^{het}FC^{het}AYDGEK (Scheme S1). The loss of 4 Da in ESI-MS (Figure S9) demonstrated that two oxidation events have taken place. Increasing the enzyme concentration to 50 μM (100 μM substrate) induced a further 2 Da mass loss (Figure S9), corresponding to the formation of one methyloxazole which is not found in arthrosiramides,¹⁹ suggesting oxazoline oxidation is kinetically hindered. Steady-state kinetics of ThcOx were carried out using full-length and trypsin-cleaved (leaderless) PatE3’ that have been heterocyclised by MicD (Figure 3, Table 1). We observed a seven-fold increase in *k*_{cat} and a 50-fold increase in *k*_{cat}/*K*_m when the leaderless peptide as opposed to the full-length substrate was used. As the leader sequence of PatE3’ is similar but not identical (Figure S2) to that of ThcE, we tested the activity of ThcOx against one of its native substrates, ThcE1. Catalytic activity towards this substrate was similar with that to PatE3’ confirming the leader does not accelerate catalytic activity.

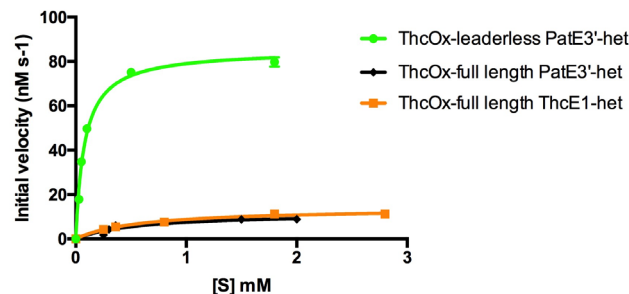


Figure 3 Initial rates of ThcOx reaction with leaderless and full-length substrates. Error bars represent the standard deviation from the mean (n = 2). Kinetic values derived from these plots are shown in Table 1.

Table 1 Catalytic parameters obtained from steady-state kinetic studies of ThcOx.

Substrate	k_{cat} (s^{-1})	K_{m} (mM)	$k_{\text{cat}}/K_{\text{m}}$ ($\text{s}^{-1}\text{M}^{-1}$)
Full ThcE1	0.14 ± 0.01	0.58 ± 0.06	240 ± 60
Full PatE3'	0.12 ± 0.01	0.57 ± 0.18	210 ± 180
Leaderless PatE3'	0.85 ± 0.02	0.08 ± 0.01	10630 ± 20

Oxidation Proceeds in a Defined N-to-C Order

^1H , ^{15}N -HSQC NMR spectroscopy was employed to investigate the oxidation order of doubly heterocyclised leaderless PatE2K (Figure 4). Heterocyclised cysteines C47 and C51 were not observed in the HSQC spectra, due to the loss of their amide protons, oxidation however alters the chemical environment of neighbouring residues A46, I48, T49, F50, A52, Y53, D54 and G55. Spectra were recorded before the addition of ArtGox, and at regular intervals afterwards. At 20 °C, the first oxidation at C47 happened rapidly after the addition of enzyme, and completed within 20 min, as demonstrated by shifting of the cross-peaks assigned to A46, I48, T49 and F50. The second oxidation step was slower and chemical shift changes corresponding to it (changes in F50, A52, Y53, D54 and G55) only became visible after 1 h of reaction. The second reaction was complete within 16 h yielding the final product (Figure 4). The same N-C order of oxidation was shown when ArtGox was reacted with full-length PatE2K (Figure S10, S11). The consistency indicates that the reaction order is an intrinsic property of ArtGox and the core substrate sequence. Consistent with the kinetic assays (Figure 3, Table 1), the reaction was clearly slower with the full-length substrate, with the first step taking nearly 12 h and complete oxidation taking 60 h.

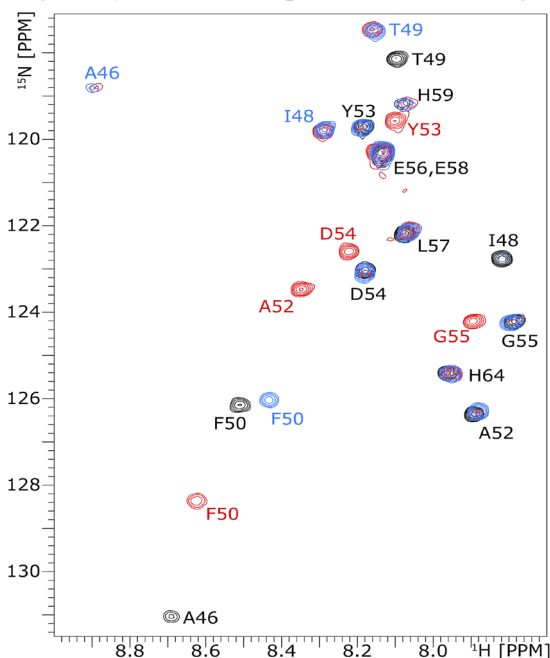


Figure 4 NMR experiment tracing the oxidation of leaderless PatE2K-2het. ^1H , ^{15}N -HSQC spectra were recorded for doubly heterocyclised, leaderless PatE2K (black), and after it was reacted with ArtGox for 20 min (blue) and 16 h (red). Cross-peaks are annotated with their residue sequences as of the full-length substrate; the colour of a label corresponds to the spectrum where the cross-peak it designates first appears. Note the cross-peaks for A46 after 20 min and 16 h are aliased in the ^{15}N dimension; the actual ^{15}N chemical shift for these signals is 133.8 ppm.

N-terminal Domains Maintains Structural Integrity and Enzyme Activity

As full-length peptides were worse substrates of the oxidase than their leaderless counterparts, we sought to determine if leader peptide binds in a way that reduces enzyme activity. PatE3' and ThcE1 that had not been heterocyclised were used to probe the binding between the leader peptide and ThcOx. However, binding with either peptide was not observed via isothermal titration calorimetry (Figure 5), suggesting that a heterocyclised core peptide alone controls the enzyme-substrate interaction. In addition, we were unable to obtain a complex structure of ThcOx with any part of the leader peptide bound. We tested if the C-terminal domain (homologous to other TOMM oxidases) alone was sufficient for enzymatic activity. The truncated oxidase domain ThcOx-Ox2 (residue 203-473) was cloned and expressed, but it was insoluble. ThcOx-Ox (residue 233-473) was then produced (Figure S12), and purified as a colourless protein, in contrast with yellow colour of native ThcOx, which was attributed to its co-factor FMN.

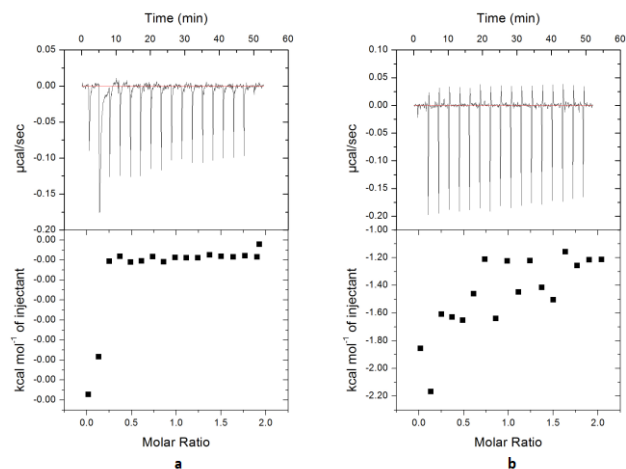


Figure 5 Calorimetric titration for the binding of peptides to ThcOx. The upper panel shows the injection of peptides (400 μM) to the cell filled with ThcOx at 20 °C, yielding an exothermic binding isotherm. The lower panel shows the integrated data obtained from the raw data, after subtracting the heat of dilution. Experimental data were fitted by using the one set of sites model from MicroCal Origin. (a) The binding of PatE3' with ThcOx. (b) The binding of ThcE1 and ThcOx.

The activity of ThcOx-ox was tested against ITAC^{Het}-ITFC^{Het}AYD, with native ThcOx as control. Whilst the native enzyme (10 μM) introduced a 4 Da mass loss in

the peptide (Figure 6d), ThcOx-Ox of the same concentration showed no activity (Figure 6b). Even with external FMN supplementation (Figure 6c) the truncated enzyme was still unable to oxidise the thiazolines within the time-scale of the experiment (16 h). The inability of exogenous FMN to rescue the reaction prompted us to think that the truncated enzyme could be unfolded or misfolded, and we therefore determined the secondary and quaternary structure of the protein with biophysical techniques. Purified ThcOx-Ox (molecular weight 27kDa) was subjected to SEC-MALS which gives a solution mass of 54 kDa (Figure 7a), consistent with that of a dimer. Circular dichroism (Figure 7b) suggested there are 30% α -helices and 20% β -sheets in the protein, similar to the 29% α -helices and 22% β -sheets among residue 233–473 shown in the crystal structure of ThcOx. Taken together, we conclude that ThcOx-Ox is folded correctly overall, but FMN binding was disrupted by the truncation.

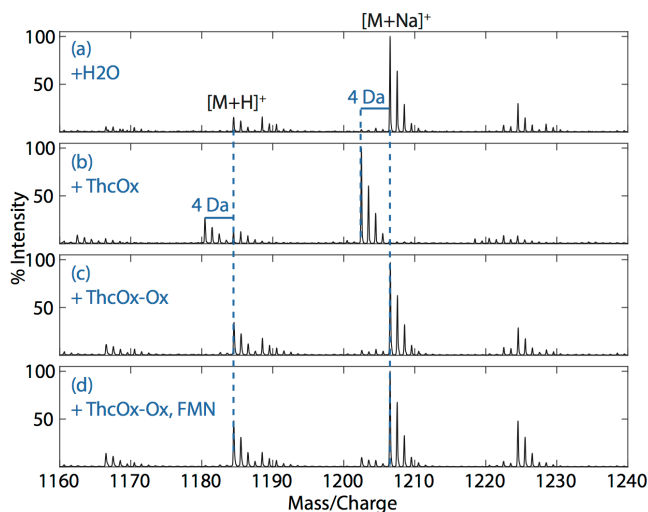


Figure 6 Mass spectra of doubly ITAC^{het}ITFC^{het}AYD (100 μ M) reacted with ThcOx and ThcOx-Ox. (a) Unoxidised peptide showing $[M+H]^+$ of 1184.5 Da and $[M+Na]^+$ of 1206.5 Da. (b) Reaction with native ThcOx resulted in a mass loss of 4 Da. (c) No mass shift was seen when the peptide was incubated with ThcOx-Ox. (d) Exogenous FMN (200 μ M) was unable to rescue the reaction.

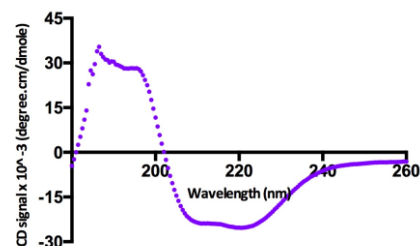
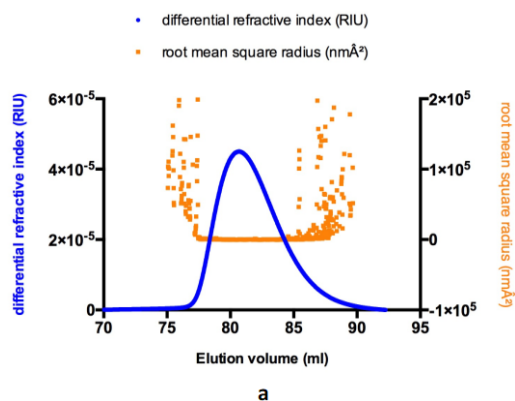


Figure 7 Biophysical analyses of ThcOx-Ox. (a) SEC-MALS chromatograph showing elution of the protein as a homogenous species. Changes in refractive index (blue) shows protein-mediated scattering of light. Root mean square radius (orange) indicates molecular size. (b) Circular dichroism spectrum of ThcOx-Ox at the concentration of 0.2 mg/ml.

Discussion

The cyanobactin oxidase is a fusion between two RiPP domain¹⁴ and an FMN-dependent oxidase domain that shows moderate sequence homology to other characterized TOMM oxidases (e.g. McbC and BalhB).^{15, 16} The RiPP domains of ThcOx each possess the characteristic structure¹⁹ of three α helices and three β strands. McbC and BalhB both form part of a heterocyclase-oxidase complex in conjunction with a RiPP (recognition) domain and a YcaO (heterocyclisation) domain. The RiPP domain has been found with a variety of activities MccB (an adenylating enzyme in Trojan horse antibiotic microcin C7 biosynthesis pathway, pdb: 3H9J), LynD (a heterocyclase in aestuaramide pathway, pdb: 4V1T) and NisB (a dehydratase in lantibiotic nisin, pdb: 4WD9).¹⁴ In many enzymes, the RiPP domain was found to be able to bind leader peptide. Since the structure of ThcOx showed it had two RiPP domains fused to an oxidase domain (B protein), we wished to investigate their role.

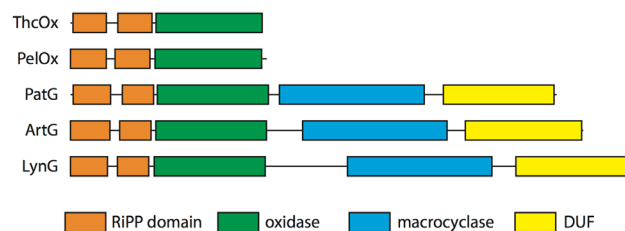


Figure 8 Domain arrangement of Cyanobactin oxidases. ThcOx and PelOx (*Nostoc* sp. *Peltigera membranacea* cyanobiont 232), standalone (putative) oxidases. PatG (*Prochloris didemni*), ArtG and LynG (*Lyngbya* sp. PCC 8106), fused oxidases. DUF, domain of unknown function. Domains were assigned by the HHpred server.²⁴

Steady-state kinetics and NMR both show that oxidase is faster and more efficient in the absence of the leader

peptide on the substrate. We were unable to detect any binding of the leader to ThcOx. Our NMR results showed that the oxidase reaction proceeds with an N to C order, opposite to that demonstrated by the cyanobactin heterocyclase TruD²². Moreover, since the order is not dependent upon the leader, it is therefore a feature of the core sequence and enzyme. The RiPP domain in the oxidase does not act as a clamp for the oxidase but its loss seems to destabilise the enzyme.

In the processing of cyanobactin precursor peptide *in vivo*, the PatA protease cleaves off the leader. The lack of leader binding by the oxidase (as well as the inefficient processing of such a leader substrate) would suggest that heterocyclisation is followed by protease cleavage (a slow reaction *in vitro*), then oxidation which we have shown is much more rapid than macrocyclisation *in vitro*. Quite why the organism uses rates to regulate production is unclear, but we note the frequent presence of epimerised amino acids adjacent to the thiazoles in the many cyanobactins. Since epimerisation has been assumed to be spontaneous for thiazolines, it may be the slow enzyme rate may be related to this. The inactivity of the RiPP domains was an unexpected result given that they are found as part of the oxidase in many cyanobactin biosynthetic pathways, and cautions against automatic assignment of function.

From a biotechnological perspective, the oxidase is a versatile enzyme capable of using a range of different substrates, including linear and macrocyclic peptides.²⁰ Its functional independence of the leader means it could be incorporated into the semi-synthetic approach toward patellamide-like peptides described in previous studies.^{18, 19}

ASSOCIATED CONTENT

Supporting Information. Figure S1 to S12, Schemes S1 and S2 and Tables S1 and S2 are supplied in the accompany supporting information. The Supporting Information is available free of charge on the ACS Publications website.

AUTHOR INFORMATION

Corresponding Author

*Telephone: +44 1334 463 792. Fax: +44 1334 467 229. E-mail: naismith@strubi.ox.ac.uk.

Author Contributions

SG, YG, US and JHN performed experiments, analysed data and wrote the paper. AFB had carried out the initial experiments. All authors have given approval to the final version of the manuscript.

‡These authors contributed equally.

Funding Sources

No competing financial interests have been declared. The work is supported by ERC grant NCB-TNT (339367).

ACKNOWLEDGMENT

We thank Dr. Clarissa Czekster for assistance with kinetics, Dr Wael Houssen (University of Aberdeen) for providing the genes *artG* and *thcOX*, Dr Huangting Liu for the vector pEHISTEVSUMO vector.²⁰

ABBREVIATIONS

ThcOx	oxidase from <i>Cyanothece</i> PCC7425 involved in cyanothecamide biosynthesis
ArtGox	oxidase domain from <i>Arthrosira spirulina</i> involved in arthrospiramide biosynthesis
HSQC spectra	heteronuclear single-quantum correlation spectroscopy
ESI-MS	electrospray ionization mass spectrometry
ITC	isothermal titration calorimetry
NMR	nuclear magnetic resonance

REFERENCES

- (1) Hong, J., and Luesch, H. (2012) Largazole: from discovery to broad-spectrum therapy. *Nat. Prod. Rep.* 29, 449–456.
- (2) Yamada, K., Kodaira, M., Shinoda, S., Komagoe, K., Oku, H., Katakai, R., Katsu, T., and Matsuo, I. (2011) Structure–activity relationships of gramicidin S analogs containing (β-3-pyridyl)-α,β-dehydroalanine residues on membrane permeability. *Medchemcomm* 2, 644.
- (3) Schreiber, S. L., and Crabtree, G. R. (1992) The mechanism of action of cyclosporin A and FK506. *Immunol. Today* 13, 136–142.
- (4) Namjoshi, S., and Benson, H. A. E. (2010) Cyclic peptides as potential therapeutic agents for skin disorders. *Biopolymers* 94, 673–680.
- (5) Davies, J. S. (2003) The cyclization of peptides and depsipeptides. *J. Pept. Sci.* 9, 471–501.
- (6) Ehrlich, A., Heyne, H.-U., Winter, R., Beyermann, M., Haber, H., Carpino, L. A., and Bienert, M. (1996) Cyclization of all-L-Pentapeptides by Means of 1-Hydroxy-7-azabenzotriazole-Derived Uronium and Phosphonium Reagents. *J. Org. Chem.* 61, 8831–8838.
- (7) Nielsen, D. S., Hoang, H. N., Lohman, R.-J., Hill, T. A., Lucke, A. J., Craik, D. J., Edmonds, D. J., Griffith, D. A., Rotter, C. J., Ruggeri, R. B., Price, D. A., Liras, S., and Fairlie, D. P. (2014) Improving on Nature: Making a Cyclic Heptapeptide Orally Bioavailable. *Angew. Chemie Int. Ed.* 53, 12059–12063.
- (8) Schmidt, E. W., Nelson, J. T., Rasko, D. a, Sudek, S., Eisen, J. a, Haygood, M. G., and Ravel, J. (2005) Patellamide A and C biosynthesis by a microcin-like pathway in *Prochloron didemni*, the cyanobacterial symbiont of *Lissoclinum patella*. *Proc. Natl. Acad. Sci. U. S. A.* 102, 7315–7320.
- (9) Czekster, C. M., Ge, Y., and Naismith, J. H. (2016) Mechanisms of cyanobactin biosynthesis. *Curr. Opin. Chem. Biol.* 35, 80–88.
- (10) Katritzky, A. R. (2010) Handbook of heterocyclic chemistry. Elsevier.
- (11) Houssen, W. E., and Jaspars, M. (2010) Azole-based cyclic peptides from the sea squirt *Lissoclinum patella*: Old scaffolds, new avenues. *ChemBioChem* 11, 1803–1815.
- (12) Hawkins, C. J., Lavin, M. F., Marshall, K. A., Van den Brenk, A. L., and Watters, D. J. (1990) Structure-activity relationships of the lissoclinamides: cytotoxic cyclic peptides from the ascidian *Lissoclinum patella*. *J. Med. Chem.* 33, 1634–1638.
- (13) Melby, J. O., Nard, N. J., and Mitchell, D. A. (2011) Thiazole/oxazole-modified microcins: complex natural products from ribosomal templates.

- (14) Burkhart, B. J., Hudson, G. A., Dunbar, K. L., and Mitchell, D. A. (2015) A prevalent peptide-binding domain guides ribosomal natural product biosynthesis. *Nat. Chem. Biol.* 11, 564–570.
- (15) Li, Y. M., Milne, J. C., Madison, L. L., Kolter, R., and Walsh, C. T. (1996) From peptide precursors to oxazole and thiazole-containing peptide antibiotics: microcin B17 synthase. *Science* 274, 1188–93.
- (16) Melby, J. O., Dunbar, K. L., Trinh, N. Q., and Mitchell, D. A. (2012) Selectivity, Directionality, and Promiscuity in Peptide Processing from a *Bacillus* sp. Al Hakam Cyclodehydratase. *J. Am. Chem. Soc.* 134, 5309–5316.
- (17) Bent, A. F., Mann, G., Houssen, W. E., Mykhaylyk, V., Duman, R., Thomas, L., Jaspars, M., Wagner, A., and Naismith, J. H. (2016) Structure of the cyanobactin oxidase ThcOx from *Cyanothece* sp. PCC 7425, the first structure to be solved at Diamond Light Source beamline I23 by means of S-SAD. *Acta Crystallogr. Sect. D Struct. Biol.* 72, 1174–1180.
- (18) Koehnke, J., Mann, G., Bent, A. F., Ludewig, H., Shirran, S., Botting, C. H., Lebl, T., Houssen, W. E., Jaspars, M., and Naismith, J. H. (2015) Structural analysis of leader peptide binding enables leader-free cyanobactin processing. *Nat. Chem. Biol.* 11, 558–563.
- (19) Houssen, W. E., Bent, A. F., McEwan, A. R., Pieiller, N., Tabudravu, J., Koehnke, J., Mann, G., Adaba, R. I., Thomas, L., Hawas, U. W., Liu, H., Schwarz-Linek, U., Smith, M. C. M., Naismith, J. H., and Jaspars, M. (2014) An Efficient Method for the In Vitro Production of Azol(in)e-Based Cyclic Peptides. *Angew. Chemie Int. Ed.* 53, 14171–14174.
- (20) Liu, H., and Naismith, J. H. (2009) A simple and efficient expression and purification system using two newly constructed vectors. *Protein Expr. Purif.* 63, 102–111.
- (21) Studier, F. W. (2005) Protein production by auto-induction in high-density shaking cultures. *Protein Expr. Purif.* 41, 207–234.
- (22) Koehnke, J., Bent, A. F., Zollman, D., Smith, K., Houssen, W. E., Zhu, X., Mann, G., Lebl, T., Scharff, R., Shirran, S., Botting, C. H., Jaspars, M., Schwarz-Linek, U., and Naismith, J. H. (2013) The cyanobactin heterocyclase enzyme: a processive adenylase that operates with a defined order of reaction. *Angew. Chem. Int. Ed. Engl.* 52, 13991–6.
- (23) Foltá-Stogniew, E. (2006) Oligomeric States of Proteins Determined by Size-Exclusion Chromatography Coupled With Light Scattering, Absorbance, and Refractive Index Detectors, in *New and Emerging Proteomic Techniques*, pp 97–112. Humana Press, New Jersey.
- (24) Soding, J., Biegert, A., and Lupas, A. N. (2005) The HHpred interactive server for protein homology detection and structure prediction. *Nucleic Acids Res.* 33, W244–W248.

SYNOPSIS Characterization of the oxidase enzyme involved in patellamide biosynthesis shows that despite the presence of a RiPP domain, the enzyme does not bind the leader of the peptide substrates.

Oxidation of cyanobactin precursor peptide is independent of leader peptide and operates in a defined order.

Sisi Gao^{‡1,2}, Ying Ge^{‡1}, Andrew F Bent^{1^}, Ulrich Schwarz-Linek¹, James H Naismith^{2,3*}

¹ Biomedical Sciences Research Complex, University of St Andrews, St Andrews, Fife KY16 9ST UK

² Research Complex at Harwell, Didcot, Oxon, OX11 0FA UK

³ Division of Structural Biology, University of Oxford, Oxford, OX3 7BN UK

[^] Deceased

^{*} To whom correspondence should be addressed

[‡] These authors contributed equally to the work

